

## Supplementary information

### **Band-bending induced passivation: high performance and stable perovskite solar cells using perhydropoly(silazane) precursor**

Hiroyuki Kanda<sup>a</sup>, Naoyuki Shibayama<sup>b</sup>, Aron Joel Huckaba<sup>a</sup>, Yonghui Lee<sup>a</sup>,

Sanghyun Paek<sup>a</sup>, Nadja Klipfel<sup>a</sup>, Cristina Roldán Carmona<sup>a</sup>, Valentin Ianis Emmanuel Queloz<sup>a</sup>,

Giulia Grancini<sup>a</sup>, Yi Zhang<sup>a</sup>, Mousa Abuhelaiqa<sup>a</sup>, Kyung Taek Cho<sup>a</sup>,

Mo Li<sup>c,d</sup>, Mounir Driss Mensi<sup>a</sup>, Sachin Kinge,<sup>e</sup> and Mohammad Khaja Nazeeruddin<sup>a\*</sup>

Corresponding author: [mdkhaja.nazeeruddin@epfl.ch](mailto:mdkhaja.nazeeruddin@epfl.ch) (Mohammad Khaja Nazeeruddin)

<sup>a</sup> Group for Molecular Engineering of Functional Materials, École Polytechnique Fédérale de Lausanne, Valais Wallis, CH-1951 Sion, Switzerland.

<sup>b</sup> Department of General Systems Studies, Graduate School of Arts and Sciences, The University of Tokyo, 3-8-1 Komaba, Meguro-ku, Tokyo 153-8902, Japan.

<sup>c</sup> Laboratory of Materials for Renewable Energy, École Polytechnique Fédérale de Lausanne, Valais Wallis, CH-1951 Sion, Switzerland.

<sup>d</sup> Swiss Federal Laboratories for Materials Science and Technology, CH-8600 Dübendorf, Switzerland.

<sup>e</sup> Toyota Motor Corporation, Toyota Motor Technical Centre, Advanced Technology Div., Hoge Wei 33, B-1930 Zaventem, Belgium.

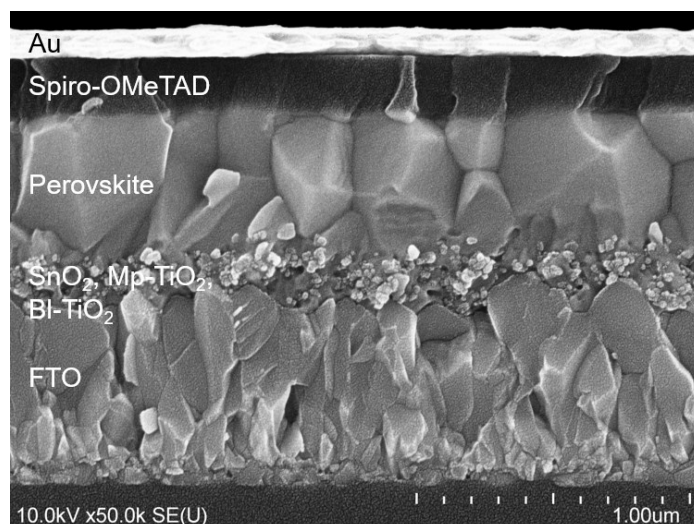


**Fig. S1** The cross-sectional SEM image of the perovskite solar cell with passivation layer. Solution concentration is 0.02 vol.%. While we expected to observe silicon oxide at the perovskite and Spiro-OMeTAD interface, we could not confirm the presence of the silica layer. The reason for this could be a too thin layer of silica.

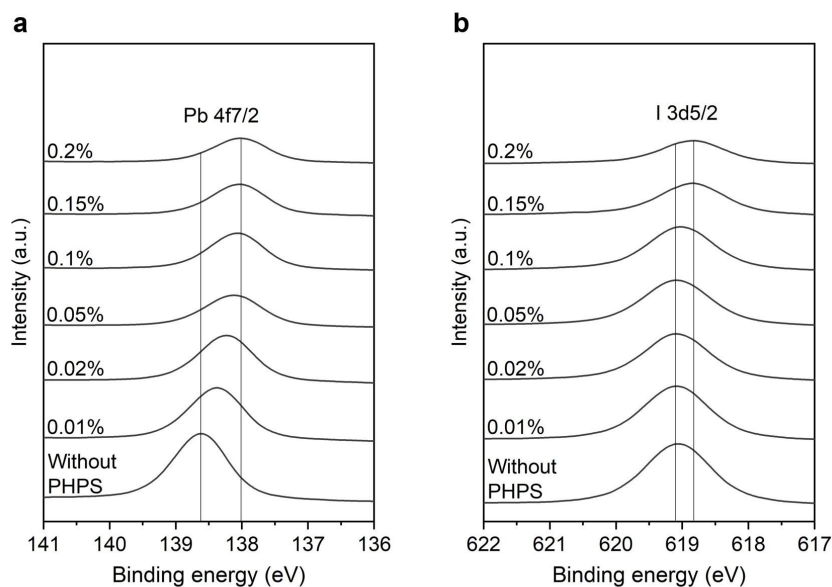


**Fig. S2** Influence of the passivation layer on the perovskite surface. XPS spectra of passivated perovskite layer of (a) Pb 4f and (b) I 3d as a function of PHPS concentration. Pb 4f peak was shifted with the increase of silicon oxide peak, while I 3d was influenced by increasing of silicon oxynitride peak (Fig. 2a).

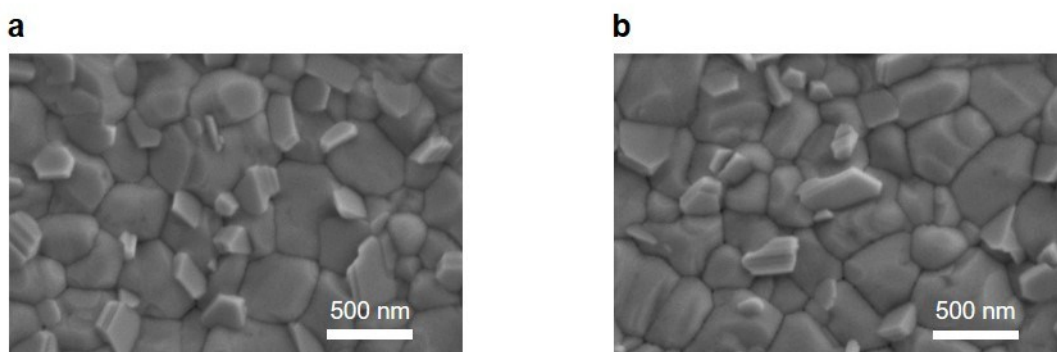


**Fig. S3** Top-view image of the perovskite absorber layer. Top-view SEM image of (a) with and (b) without PHPS treatment.

The PHPS concentration was 0.02 vol.%.

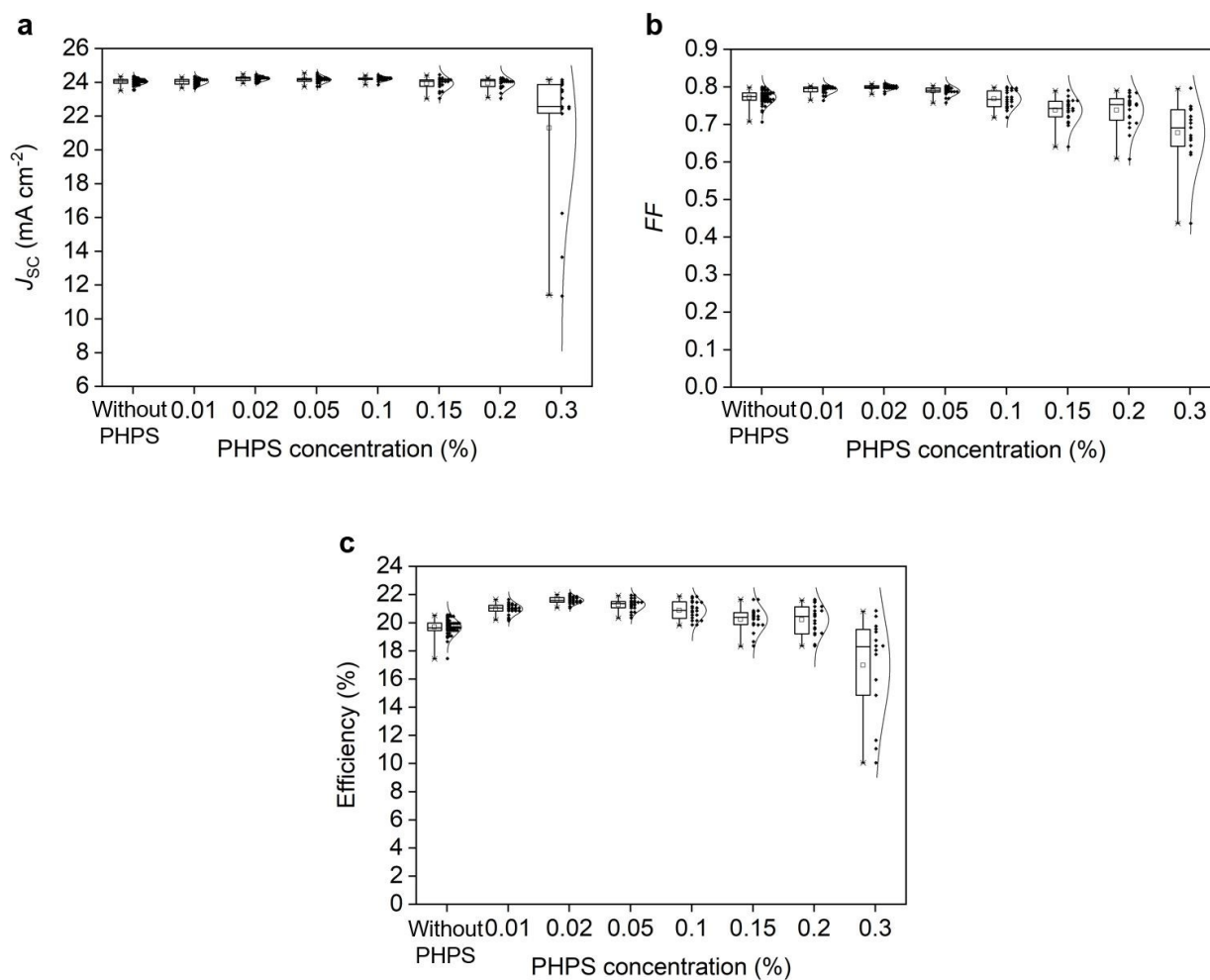


**Fig. S4** Photovoltaic property distributions of perovskite solar cells changing PHPS concentration. Distribution of photovoltaic properties for (a)  $J_{SC}$ , (b)  $FF$ , and (c) photo conversion efficiency as a function of PHPS concentration.

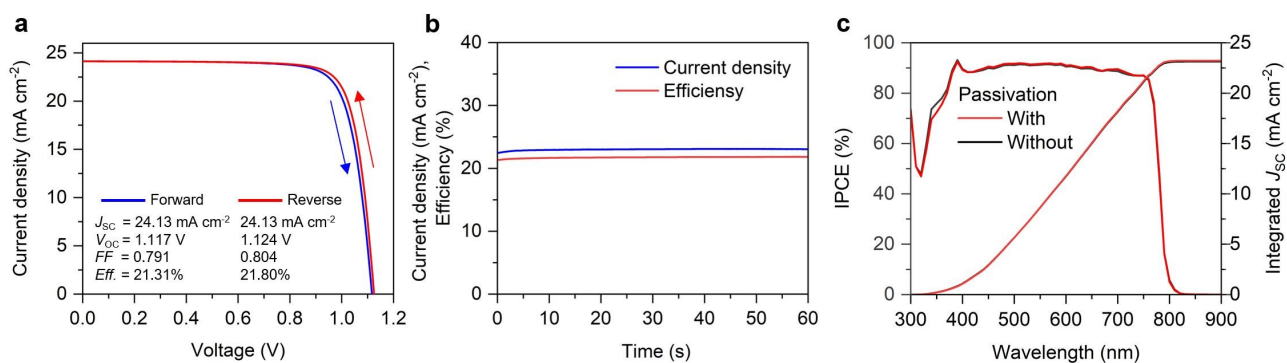
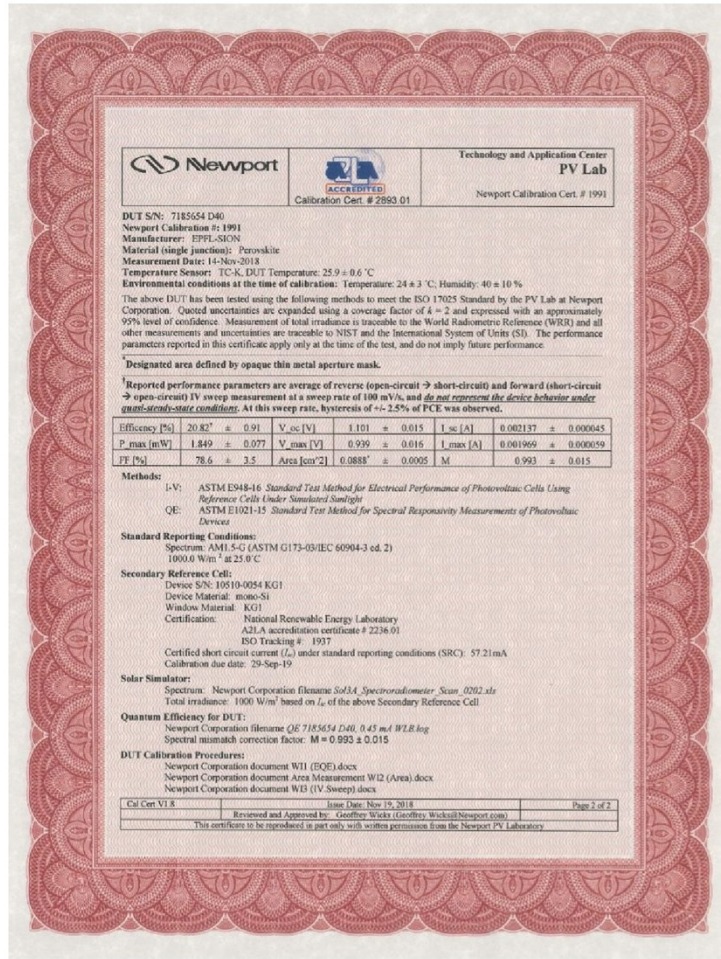
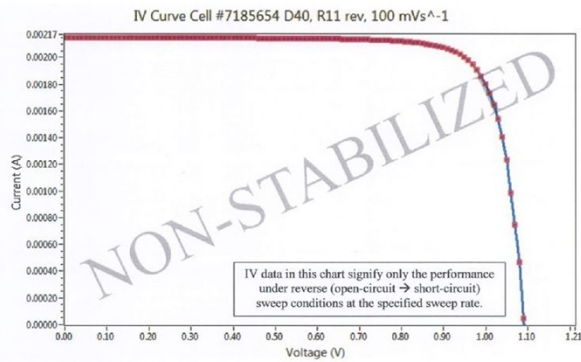


**Fig. S5** Device performances of perovskite solar cells. (a) Photovoltaic properties of  $I$ - $V$  curves for hysteresis and (b) maximum power tracking for  $J_{SC}$  and conversion efficiency with passivation. (c) IPCE spectra and integrated  $J_{SC}$  with and without passivation. PHPS concentration is 0.02 vol.%.

a



b



c

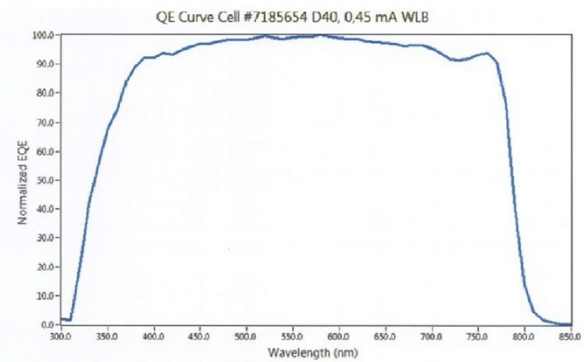


**Fig. S6** Certification result from Newport Corp. (a) Photovoltaic properties, (b) *I*-*V* curves, and (c) IPCE data for passivated PSCs using optimized conditions. The masked area was 0.0888 cm<sup>2</sup>. When the solar cell *I*-*V* curve was measured, there was no equilibrium time of light illumination, which is shown as “non-stabilized” in Fig. S6b.

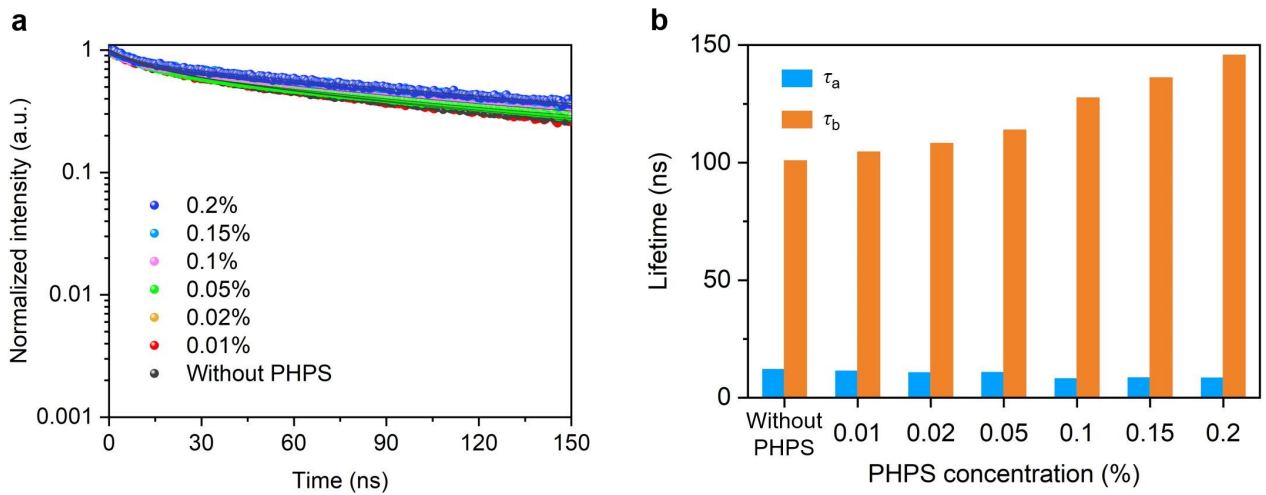


**Fig. S7** Lifetime characterization using PL measurement. (a) PL decay and (b) lifetime as a function of PHPS concentration.

The device structure is Glass/Perovskite/Passivation layer.

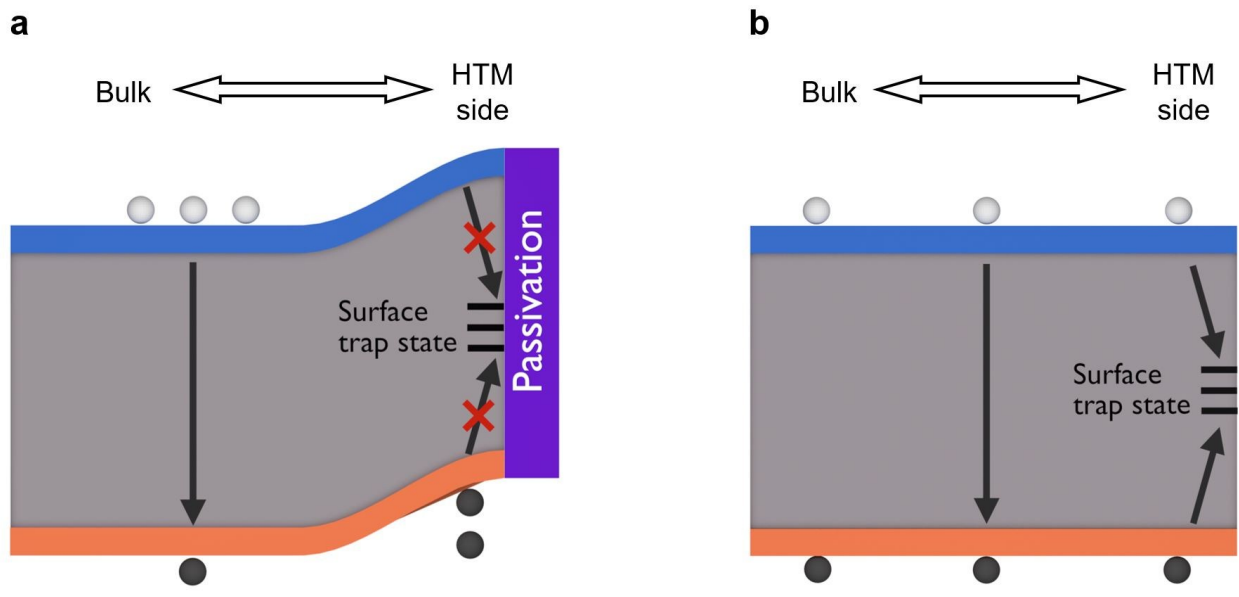


**Fig. S8** Effect of band-bending for electron-hole recombination. Perovskite layer (a) with and (b) without the passivation layer.

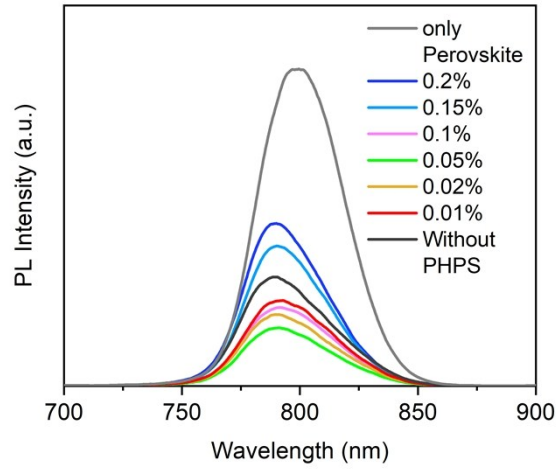


**Fig. S9** Steady-state PL spectra for Glass/Perovskite/Passivation layer/HTM structure.

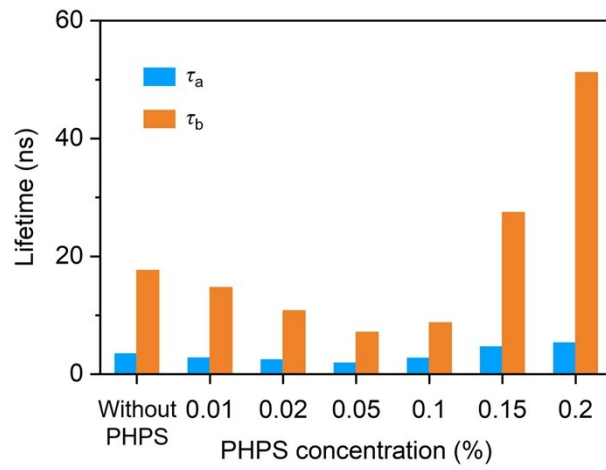


**Fig. S10** Lifetime characterization with HTM on passivation layer. Lifetime of PL decay as a function of PHPS concentration.

The device structure is Glass/Perovskite/Passivation layer/HTM.

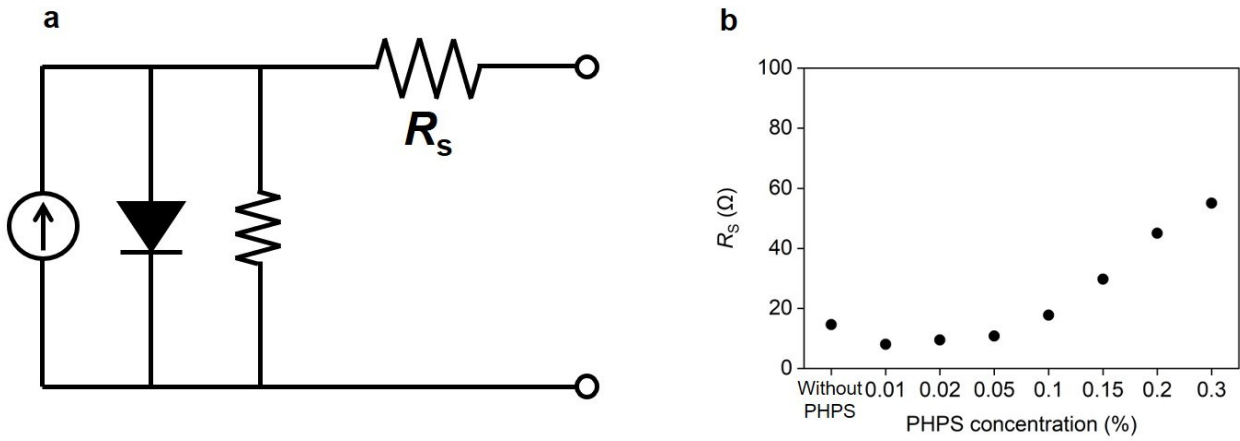


**Fig. S11** Electrical properties of perovskite solar cells for series resistance. (a) Equivalent circuit model of perovskite solar cells. (b) Average  $R_s$  as a function of PHPS concentration.

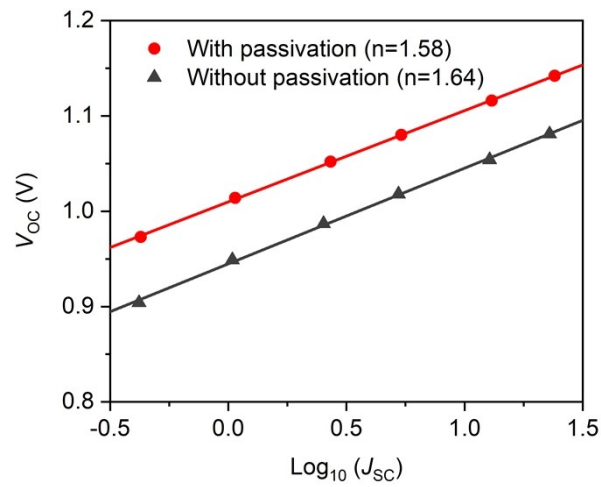


**Fig. S12** Ideal factor characterization.  $V_{OC}$  plotting as a function of the logarithm of  $J_{SC}$  of PSCs with and without passivation.

PHPS concentration is 0.02 vol.%. The ideal factor was calculated by Suns- $V_{OC}$  method.



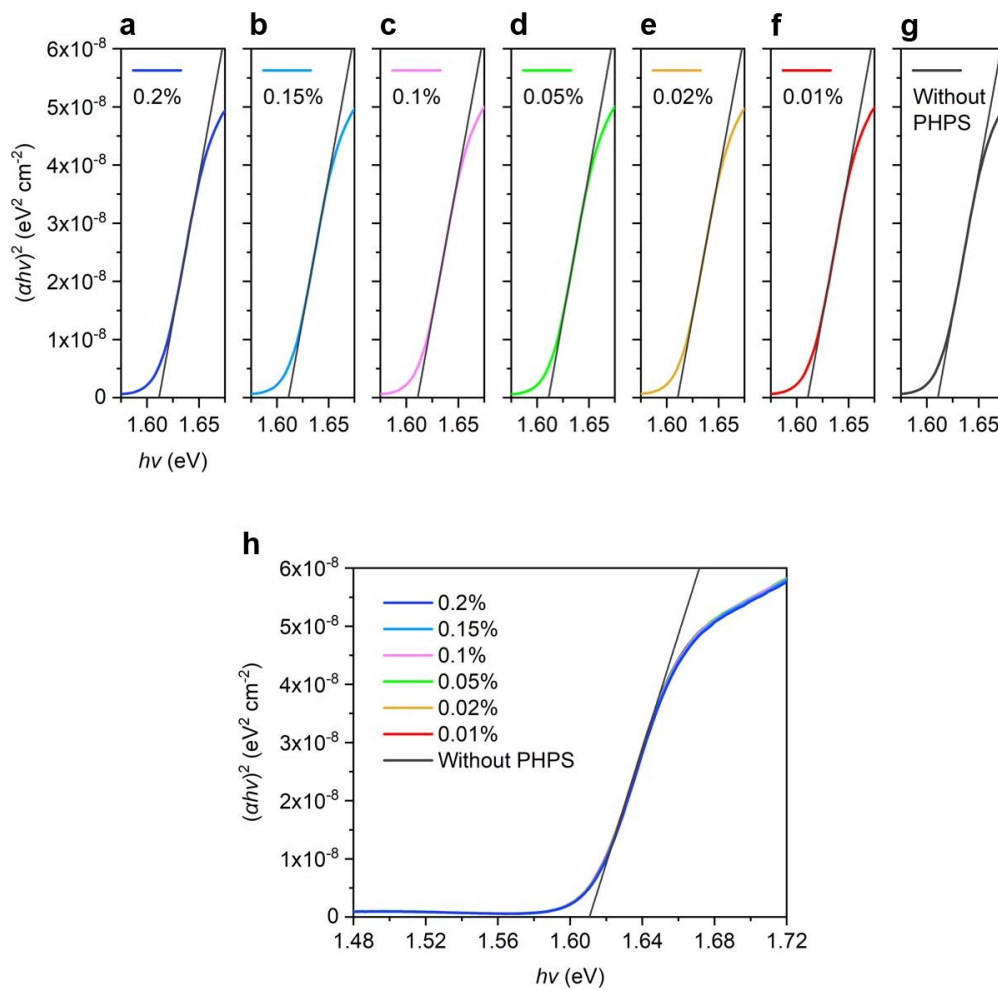


**Fig. S13** Bandgap determination. Plots of  $(\alpha h\nu)^2$  as a function of  $h\nu$  for determining bandgap of perovskite changing PHPS

concentration of (a) 0.2, (b) 0.15, (c) 0.1, (d) 0.05, (e) 0.02, (f) 0.01 vol.%, (g) without PHPS, and (h) all in one. All of the

determined bandgap was same as 1.611 eV.

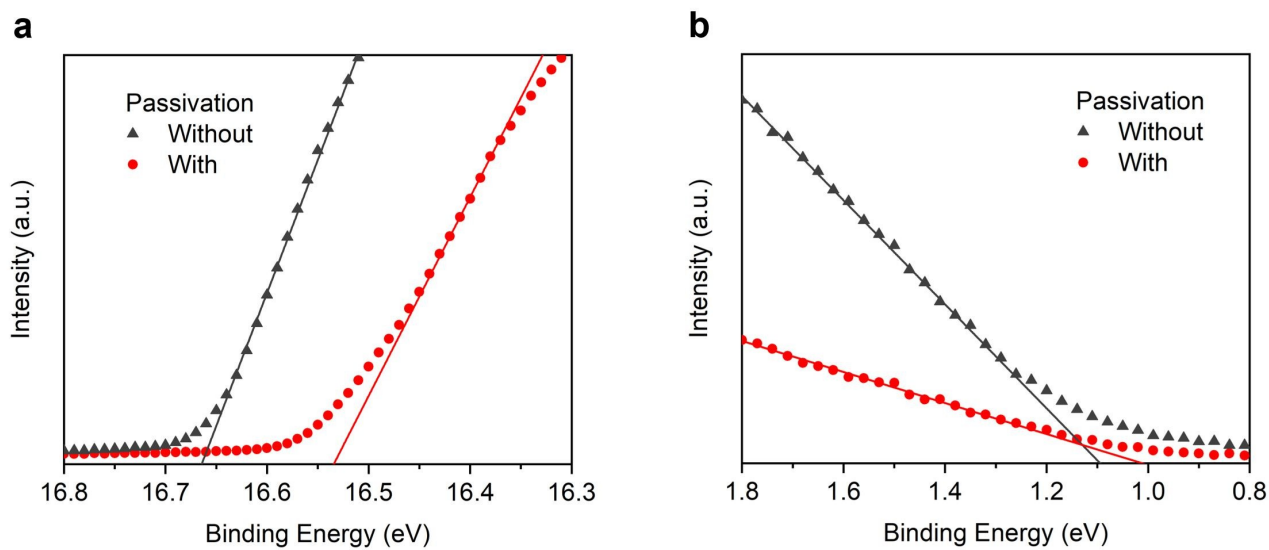


**Fig. S14** Measurement of energy band diagram parameters. (a) UPS spectrum edge of work function and (b) valence band edge of perovskite layer with and without passivation. PHPS concentration is 0.02 vol.%. Work function was calculated by subtracting 21.22 eV from the spectrum edge of Fig. S14a.

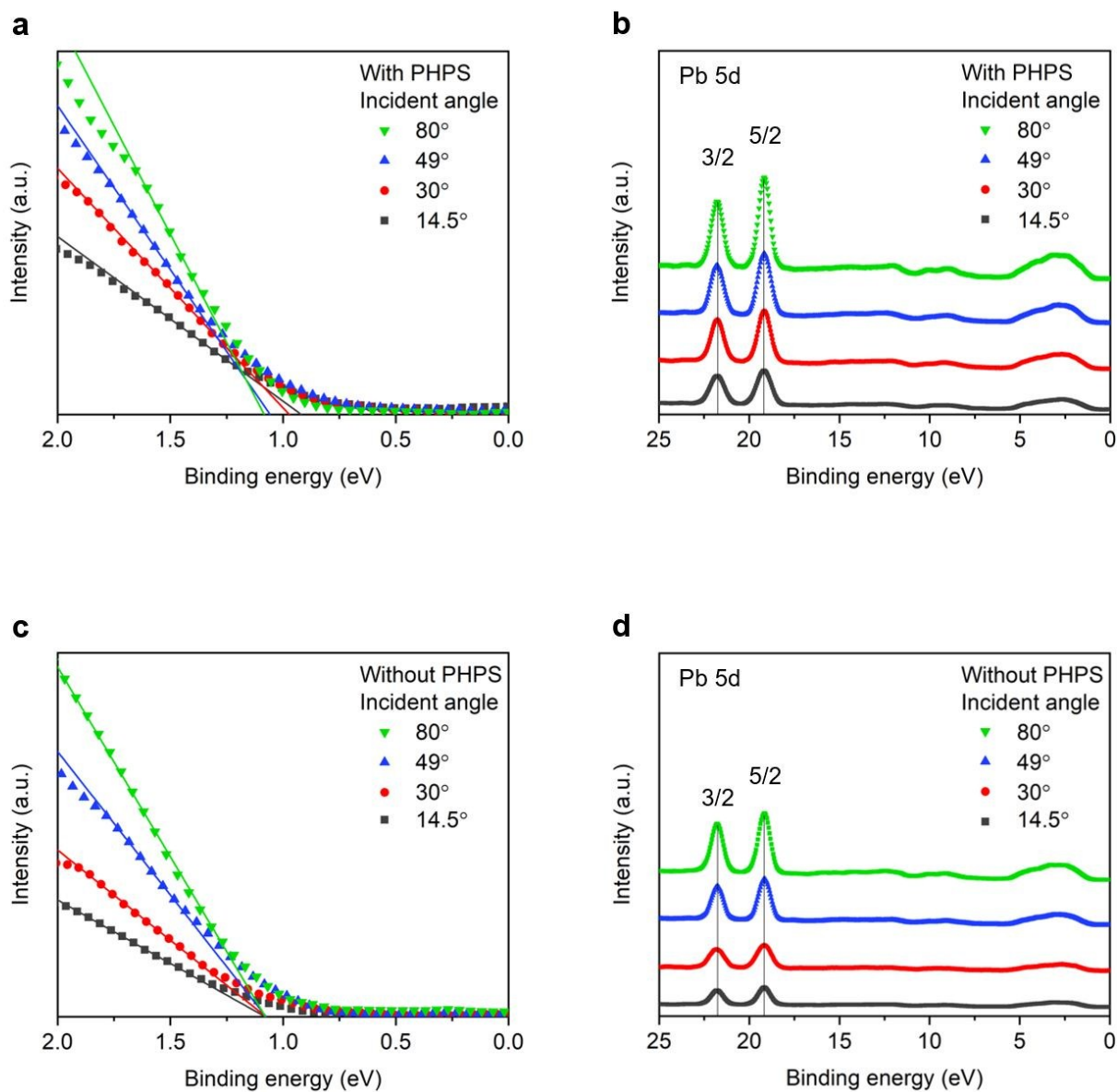


**Fig. S15** Measurement of energy band diagram parameter for surface and bulk perovskite. (a) Valence band edge of zoom-in and (b) zoom-out of perovskite with passivation was measured by AD-HAXPES with 7940 eV photon energy. (c) Valence band edge of zoom-in and (d) zoom-out of perovskite without passivation. Incident angle was changed from 14.5 to 80 degree. PHPS concentration is 0.02 vol.%.

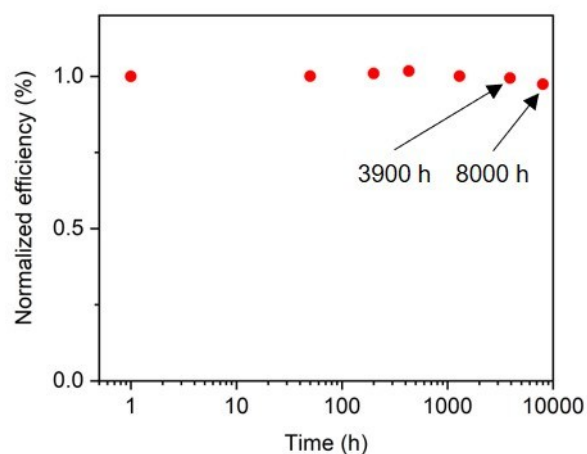


**Fig. S16** Device stability of perovskite solar cell. The efficiency of perovskite solar cells with passivation layer was normalized. PHPS concentration is 0.02 vol.%. The sample was kept in the dark in ambient dry air. The initial photovoltaic properties were  $J_{SC}=24.29 \text{ mA cm}^{-2}$ ,  $V_{OC}=1.113 \text{ V}$ ,  $FF=0.798$ , and  $Eff.=21.56\%$ .

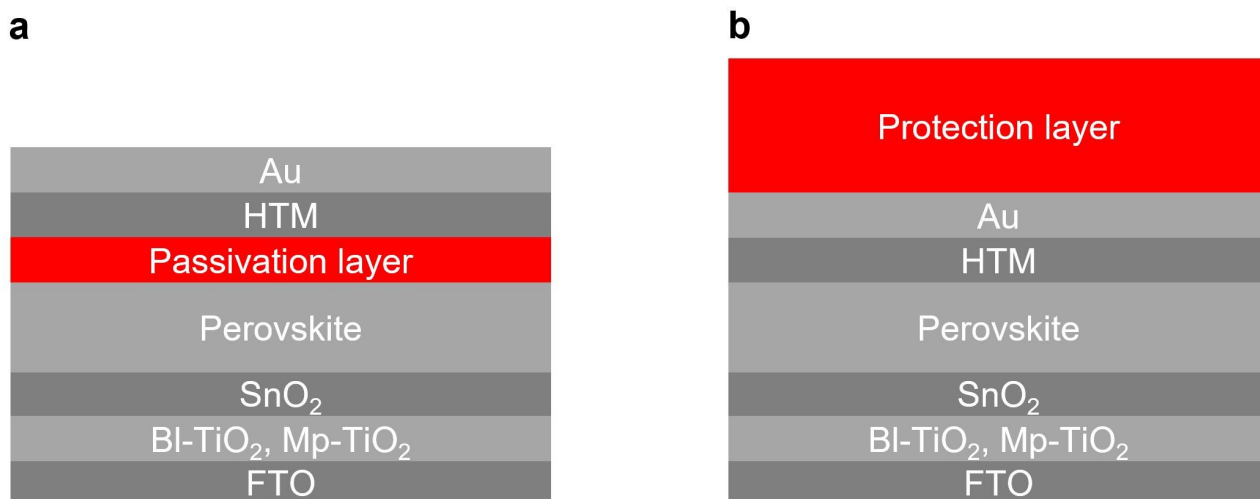


**Fig. S17** Perovskite device for waterproofing. (a) Passivated perovskite solar cell with PHPS treatment (0.01-0.3 vol.%). (b)

Perovskite solar cells with thick protection layer (500 nm) by using PHPS (20 vol.%) to obtain the waterproof effect.

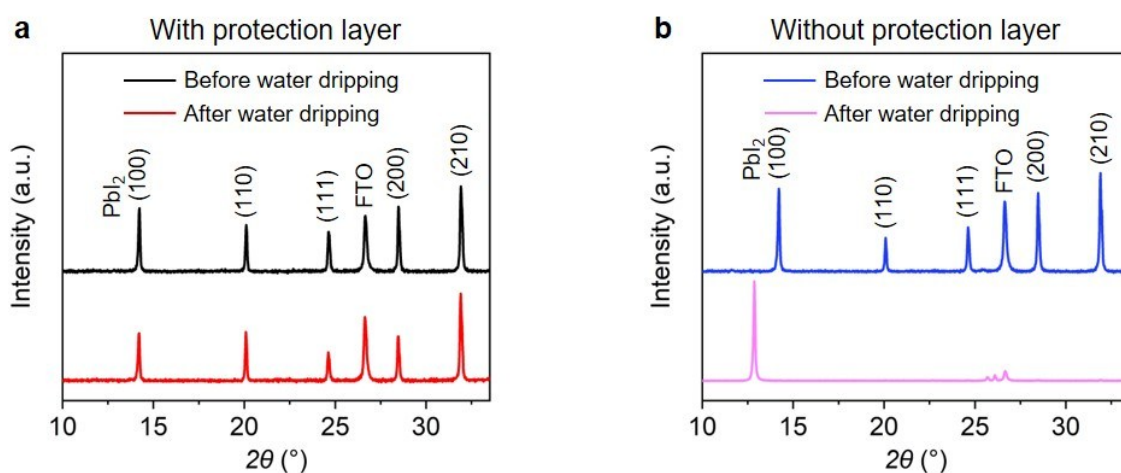


**Fig. S18** Crystallinity of perovskite layer before and after water dripping. XRD pattern (a) with and (b) without protection layer on the PSCs device. For the XRD measurement, samples were measured only in the active area by avoiding the edge of the samples. The device structure is FTO/c-TiO<sub>2</sub>/mp-TiO<sub>2</sub>/c-SnO<sub>2</sub>/Perovskite/Spiro-OMeTAD/Protection layer. PHPS concentration was 20 vol.%, which was spin-coated (3000 rpm) on Spiro-OMeTAD layer. Water (15 mL) was dropped on the devices during spin-coating (2000 rpm), then compared XRD before and after water dripping. The intensity of the XRD spectrum was normalized with the highest peak of each spectrum.

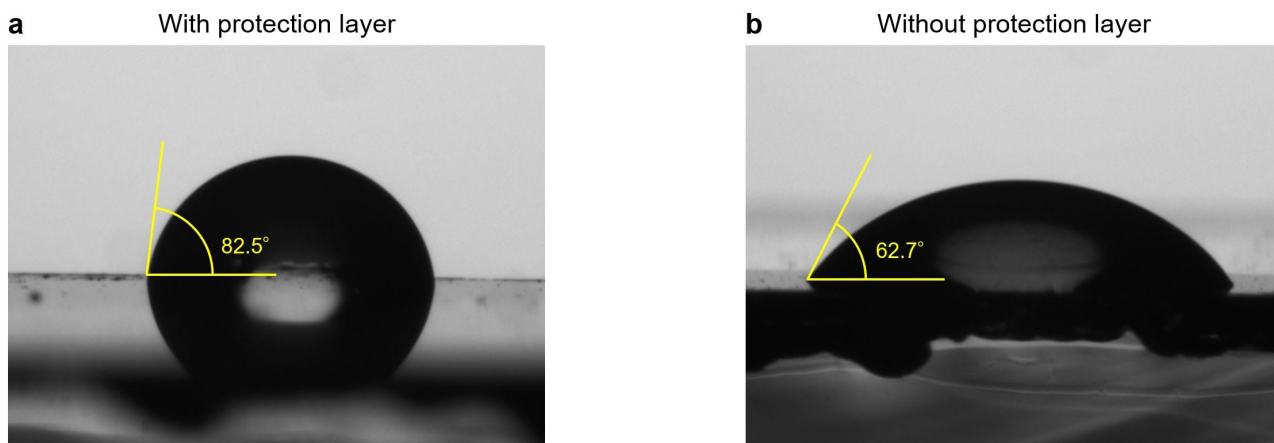


**Fig. S19** Contact angle of the device with and without protection layer. Water contact angle (a) with and (b) without protection layer on the device. Device structure is FTO/TiO<sub>2</sub>/SnO<sub>2</sub>/Perovskite/Spiro-OMeTAD/Protection layer. PHPS concentration is 20 vol.%. Spin-coating speed was 3000 rpm for PHPS deposition.

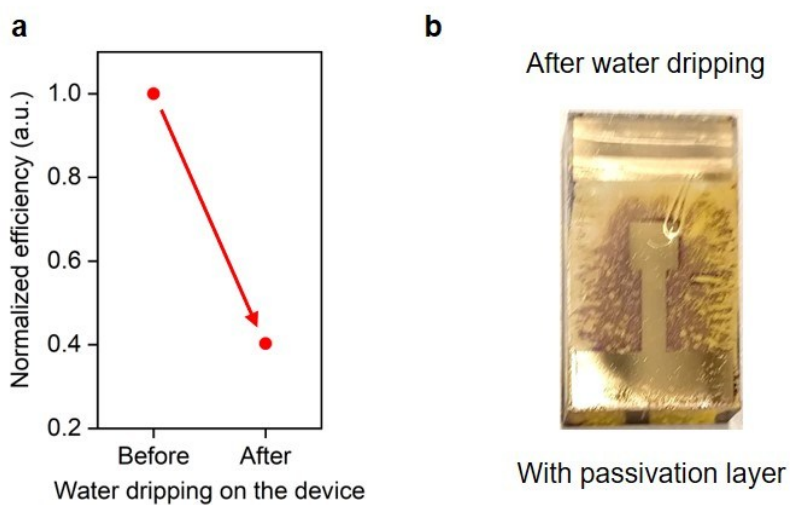


**Fig. S20** Perovskite device waterproofing. (a) Normalized efficiency before and after water dripping on the device. The structure is <FTO/TiO<sub>2</sub>/SnO<sub>2</sub>/Perovskite/Passivation layer/HTM/Au> (Fig. S17a). Water was dropped on the device during spin-coating. (b) Device images after water dripping. PHPS concentration is 0.02 vol.%.

**Table S1** Detail fitting parameters for the time-resolved photoluminescence measurement.

□	$A_1$	$\tau_a$ (ns)	$A_2$	$\tau_b$ (ns)	$A_1$	$\tau_b$ (ns)	$A_2$	$\tau_b$ (ns)
Structure	Glass/Perovskite/Passivation layer/HTM				Glass/Perovskite/Passivation layer			
Without PHPS	0.826	3.48	0.257	17.96	0.224	11.99	0.578	100.8
0.01%	0.871	2.76	0.217	14.74	0.218	11.33	0.597	104.5
0.02%	0.838	2.44	0.278	10.80	0.181	10.64	0.576	108.1
0.05%	0.976	1.91	0.277	7.12	0.272	10.74	0.566	113.8
0.10%	0.806	2.72	0.274	8.72	0.138	8.10	0.595	127.5
0.15%	0.795	4.64	0.279	27.47	0.098	8.51	0.624	136.0
0.20%	0.694	5.33	0.370	51.19	0.111	8.37	0.633	145.7

†The equation for the fitting is  $y=y_0+A_1 \times \exp(-(x-x_0)/\tau_a)+A_2 \times \exp(-(x-x_0)/\tau_b)$ .

**Table S2** Photovoltaic properties of PSCs device with and without protection layer comparing before and after water dripping.

Protection layer	Water dripping	$J_{SC}$ (mA cm <sup>-2</sup> )	$V_{OC}$ (V)	$FF$	$Eff.$ (%)
With	Before	23.97	1.051	0.770	19.42
	After	24.01	1.054	0.768	19.44
Without	Before	24.07	1.044	0.767	19.28
	After	9.07	0.967	0.563	4.94

†The structure is <FTO/TiO<sub>2</sub>/SnO<sub>2</sub>/Perovskite/HTM/Au/Protection layer> (Fig. S17b). PHPS was deposited on the completed device. PHPS concentration is 20 vol.%.

**Table S3** Photovoltaic properties of passivated PSCs device comparing before and after water dripping.

Water dripping	$J_{SC}$ (mA cm <sup>-2</sup> )	$V_{OC}$ (V)	$FF$	$Eff.$ (%)
Before	24.03	1.131	0.784	21.34
After	23.12	0.959	0.388	8.60

†The structure is <FTO/TiO<sub>2</sub>/SnO<sub>2</sub>/Perovskite/Passivation layer/HTM/Au> (Fig. S17a). Water was dropped on the device during spin-coating. PHPS was deposited on the perovskite layer for passivation. PHPS concentration is 0.02 vol.%.